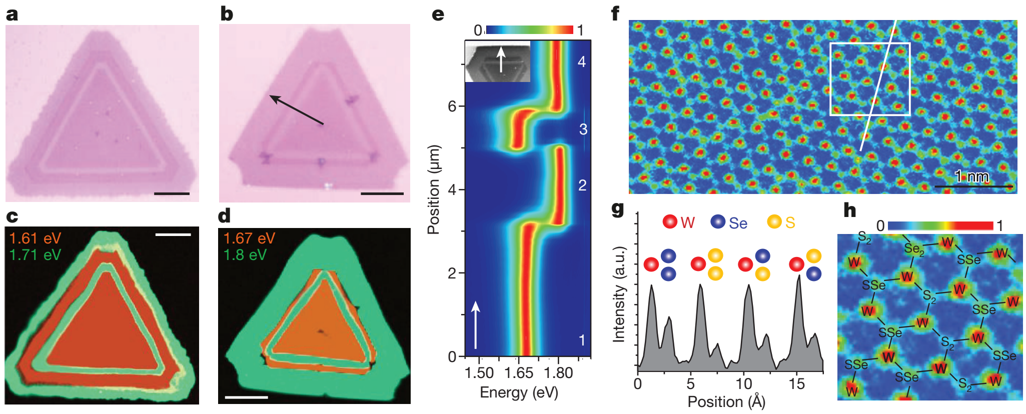

Figure 3 | Synthesis of three-junction lateral heterostructures based on MoX_2–WX_2. $X_2 = S_{2(1-n)}Se_{2n}$. **a**, **b**, Optical images of three-junction heterostructures composed of $MoS_{0.64}Se_{1.36}$–$WS_{0.68}Se_{1.32}$ (ALH1, **a**) and $MoS_{1.04}Se_{0.96}$–$WS_{1.08}Se_{0.92}$ (ALH2, **b**). **c**, **d**, Corresponding composite photoluminescence maps of ALH1 at 1.61 eV and 1.71 eV (**c**) and ALH2 at 1.6 eV and 1.8 eV (**d**). **e**, Normalized photoluminescence colour contour plot for ALH2 along a direction perpendicular to the interfaces; $\lambda_{exc} = 633$ nm. The inset shows a typical SEM image of ALH2; the width of the image corresponds to 24 μm. **f**, Atomic-resolution HAADF-STEM image of a $WS_{2(1-x)}Se_{2x}$ domain of ALH2. **g**, Electron intensity profile along the white line indicated in **f**. **h**, Magnified image of the region enclosed by the box in **f**, showing the different configurations of chalcogen sites. Scale bars, 10 μm (**a**–**d**).

constant, with sharp discontinuities at the interfaces. TEM analysis confirms that the individual domains are ternary alloys of $MoS_{2(1-x)}Se_2$ or $WS_{2(1-x)}Se_2$. Figure 3f shows a Z-contrast TEM image from a $WS_{2(1-x)}Se_{2x}$ domain. The differences in scattered electron intensities (Fig. 3g) associated with the metal sites (tungsten in this case) and with three distinct combinations of the chalcogen atoms (S_2, Se_2 or SSe) were used to identify the elemental configurations at the different atomic positions within the crystal[28] (Fig. 3h). The concentration (x) at each domain was calculated from the measured photoluminescence peak positions according to Vegard's law $E_g(MS_{2(1-x)}Se_{2x}) = (1-x)E_g(MS_2) + xE_g(MSe_2) - bx(1-x)$; where M = Mo or W and considering bandgap bowing parameters of $b = 0.05$

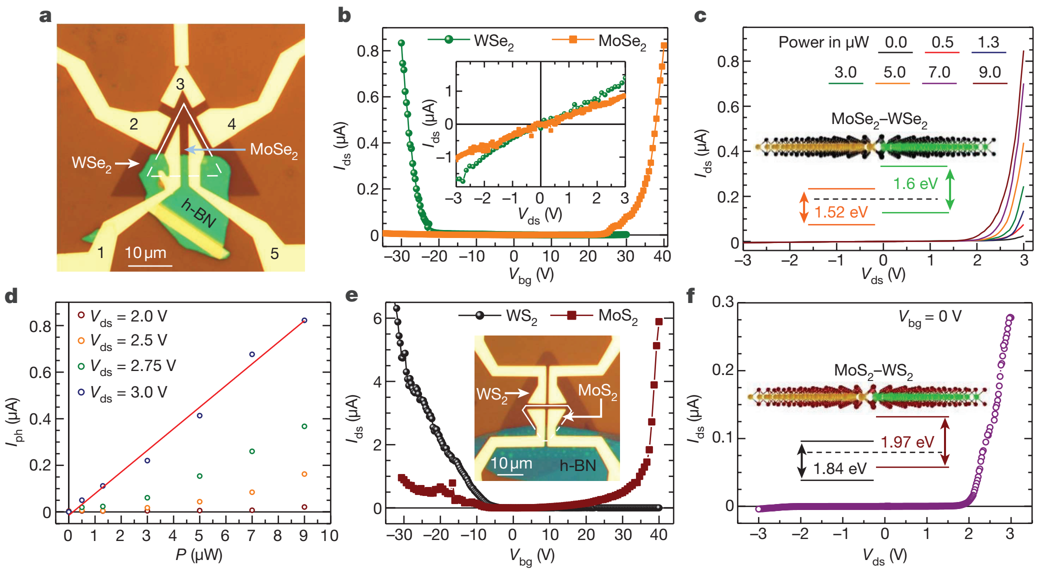

Figure 4 | Electrical characterization of the heterostructures. **a**, Micrograph of a $MoSe_2$–WSe_2 single junction grown by chemical vapour deposition, displaying the configuration of titanium and gold contacts used for the electrical characterization of the individual WSe_2 and $MoSe_2$ domains as well as the electrical transport across their junction. An exfoliated crystal of hexagonal boron nitride (h-BN) was transferred onto the lower edge of the junction to isolate contacts 1 and 5 from the WSe_2 edge, as these contacts are designed to probe only the $MoSe_2$ domain. The properties of the WSe_2 domain are probed through contacts 2 and 3 or 3 and 4. **b**, Typical drain to source current I_{ds} as a function of the gate voltage V_{bg} for the WSe_2 (green) and the $MoSe_2$ (orange) domains. The WSe_2 domain displays current mainly at negative gate voltages—that is, hole-doped-like transport—whereas the $MoSe_2$ domain displays an electron-doped-like response. The inset plots I_{ds} as a function of the bias voltage V_{ds}, showing a nearly linear dependence on V_{ds} when $V_{bg} = 0$ V. This indicates thermionic emission of charge carriers across the Schottky barriers located at the electrical contacts. **c**, I_{ds} as a function of V_{ds} across the $MoSe_2$–WSe_2 interface, displaying a typical diode-like response which becomes more prominent under illumination ($V_{bg} = 0$ V). The inset shows a sketch of the $MoSe_2$–WSe_2 domains, their interface, and respective band alignments. **d**, Photoinduced current $I_{ph} = I_{ds} - I_{dark}$, where I_{ds} is the current observed under illumination and I_{dark} is the current observed under dark conditions, as a function of the illumination power P. The red line is a linear fit, indicating a linear dependence of I_{ph} on P at high bias voltages. **e**, I_{ds} as a function of V_{bg} for a WS_2 (black) and a MoS_2 (brown) domain. Whereas WS_2 behaves as a hole-doped compound, MoS_2 displays ambipolar behaviour, albeit with a more pronounced electron-like response. The inset shows a micrograph of the MoS_2–WS_2 single junction device showing the configuration of contacts used to evaluate individual domains and their interface. **f**, I_{ds} as a function of V_{ds} across the MoS_2–WS_2 interface, showing the characteristic diode-like response. The inset shows a sketch of the MoS_2–WS_2 domains, their interface, and respective band alignments.